available at www.sciencedirect.com

ScienceDirect

journal homepage: www.elsevier.com/locate/chnjc

Article

Preparation of ternary Ag/Ag_3PO_4/g-C_3N_4 hybrid photocatalysts and their enhanced photocatalytic activity driven by visible light

Kai Shen [a,*], Mohammed Ashraf Gondal [b,#], Rashid Ghulam Siddique [b], Shan Shi [a], Siqi Wang [a], Jiangbo Sun [a], Qingyu Xu [c]

[a] *College of Materials Science and Technology, Nanjing University of Aeronautics and Astronautics, Nanjing 211100, Jiangsu, China*

[b] *Laser Research Group, Physics Department and Center of Excellence in Nanotechnology, King Fahd University of Petroleum and Minerals, Dhahran 31261, Saudi Arabia*

[c] *Department of Physics, Southeast University, Nanjing 211189, Jiangsu, China*

ARTICLE INFO

Article history:
Received 26 July 2013
Accepted 10 September 2013
Published 20 January 2014

Keywords:
Silver nanoparticle
Silver orthophosphate (Ag_3PO_4)
Graphitic carbon nitride (g-C_3N_4)
Surface plasmon resonance
Heterojunction structure

ABSTRACT

The preparation of a series of ternary Ag/Ag_3PO_4/g-C_3N_4 hybrid photocatalysts, which display enhanced photocatalytic activity, was reported. The crystal structure, morphology, composition, optical absorption, and efficient separation of charge carriers were studied by X-ray diffraction, scanning electron microscopy, absorption and photoluminescence spectroscopy measurements. Using rhodamine B as a model contaminant, the as-prepared Ag/Ag_3PO_4/g-C_3N_4 hybrid photocatalyst exhibited superior degradation performance under visible light irradiation than Ag_3PO_4 or binary Ag_3PO_4/g-C_3N_4 hybrid photocatalyst systems. The surface plasmon resonance of the 40 nm-silver nanoparticles formed on the surface of Ag_3PO_4 and the heterojunction formed at the interface between Ag_3PO_4 and g-C_3N_4, are considered to be the major physical-chemical origin and to be responsible for the enhanced photocatalytic activity.

1. Introduction

Heterogeneous photocatalysis is a promising approach to development of technology for environmental remediation, solar energy conversion, and hydrogen production. The pioneering work of Fujishima et al. [1] spurred interest in the development of visible light driven photocatalysis for application in environmental technology. Subsequent achievements [2–5] have contributed to a drive towards the development of efficient photocatalysts with high quantum efficiency in the visible portion of the solar spectrum (380–780 nm) [6].

Silver orthophosphate (Ag_3PO_4) is an active semiconductor that can take part in photooxidation processes. Ag_3PO_4 also has a quantum efficiency of 90% at wavelengths longer than 420 nm [7] and shows high photocatalytic activity owing to its absorption in the visible portion of the solar spectrum and high charge carrier mobility. This is because of the delocalized charge distribution of the conduction-band minimum, which results in a small electron effective mass, which is beneficial for the surface carrier mobility [8].

Graphitic carbon nitride (g-C_3N_4) is based on the stacked two-dimensional structure analogous of graphite with N replacing non-adjacent carbon atoms. This material has drawn attention for its potential in water splitting application as a

* Corresponding author. Tel/Fax: +86-25-84895871; E-mail: shenkai84@nuaa.edu.cn
# Corresponding author. Tel: +966-3-8602351; Fax: +966-3-8604281; E-mail: magondal@kfupm.edu.sa

This work was supported by the National Natural Science Foundation of China (51172044) and the Project R15-CW-11 (MIT11109, MIT11110) by KFUPM (King Fahd University of Petroleum and Minerals).
DOI: 10.1016/S1872-2067(12)60712-8 | http://www.sciencedirect.com/science/journal/18722067 | Chin. J. Catal., Vol. 35, No. 1, January 2014

metal-free photocatalyst operating under visible light irradiation, as reported by Wang et al. [9]. However, the potential of this material is limited by inherent constraints such as inefficient use of the visible portion of the solar spectrum and a high electron/hole recombination rate. The photocatalytic efficiency of g-C_3N_4 needs further enhancement prior to any practical application. Various g-C_3N_4 based hybrid photocatalysts including g-C_3N_4/$BiPO_4$ [10], graphene/g-C_3N_4 [11], g-C_3N_4/Bi_2WO_6 [12], Fe-g-C_3N_4-LUS-1 [13], g-C_3N_4/SiO_2-HNb_3O_8 [14], and g-C_3N_4/TaON [15] have been developed to further extend the visible light absorption range and the photogenerated carriers separation efficiency.

Described herein is a simple photochemical precipitation based preparation of a series of novel ternary Ag/Ag_3PO_4/g-C_3N_4 hybrid photocatalysts and a detailed investigation of the catalytic activity using rhodamine B (RhB) as a model contaminant. Our photocatalytic experiments indicate that the Ag/Ag_3PO_4/g-C_3N_4 hybrid system exhibits superior photocatalytic performance for RhB degradation compared with a binary Ag_3PO_4/g-C_3N_4 photocatalyst, or Ag_3PO_4 and g-C_3N_4 as individual components. It was found that RhB photodegradation strongly depends on the proportion of silver nanoparticles on the Ag_3PO_4 surface and the ratio of the components in the Ag_3PO_4/g-C_3N_4 hybrid. The enhanced photoactivity can be attributed to the surface plasmon resonance (SPR) originating from silver nanoparticles and the heterojunction-like interface between Ag_3PO_4 and g-C_3N_4. This work is a continuation of our commitment to developing environmentally friendly technologies for clean fuel by using the photocatalytic technique [16–21].

2. Experimental

2.1. Materials

All the chemicals used in this study were of analytical grade and used as received without further purification. Absolute ethanol (C_2H_5OH), sodium bismuthate ($NaBiO_3$), disodium hydrogen phosphate (Na_2HPO_4), anatase-TiO_2, and rhodamine B (RhB) were purchased from Sinopharm Chemical Reagent Co. Melamine and silver nitrate ($AgNO_3$) were obtained from Shanghai Lingfeng Chemical Reagent Co. Ltd and Jiangsu Qiangsheng Chemical Co. Ltd, respectively. Distilled water was produced using a Direct-Q Millipore filtration system to a resistivity of 18.2 MΩcm (Millipore Limited, Watford, UK).

2.2. Preparation

g-C_3N_4 was prepared through a pyrolysis process using melamine as the starting material [22], and then binary Ag_3PO_4/g-C_3N_4 (x) (where x denotes the mass fraction of Ag_3PO_4 in the sample) hybrid photocatalysts were prepared by a chemical deposition-precipitation method. In a typical preparation for the case of Ag_3PO_4/g-C_3N_4 (0.8), 2.3 g of g-C_3N_4 was dispersed into an aqueous solution of $AgNO_3$ (1.26 g/50 mL). Then a solution of Na_2HPO_4 (0.9 g/50 mL) was added drop-wise over 30 min into the above suspension with stirring until the precipitation was completed. The mixture was then centrifuged, washed with water, and dried overnight at 50 °C. The obtained Ag_3PO_4/g-C_3N_4 (0.8) powder (2.0 g) was dispersed in 200 mL of water and irradiated by a 300 W Xenon lamp (Beijing Trusttech Co. Ltd., PLS-SXE-300) equipped with a visible light band pass filter (400–800 nm) for 0.5–3 h. The final product was collected by centrifugation at 4000 r/min, washed with absolute ethanol/water several times, and then dried at 50 °C. The series of Ag/Ag_3PO_4/g-C_3N_4 hybrid photocatalysts were denoted Ag/Ag_3PO_4/g-C_3N_4 (x; t), where t is the irradiation time (0.5–3 h) for the preparation.

2.3. Characterization

The crystal structure of the ternary Ag/Ag_3PO_4/g-C_3N_4 hybrid photocatalysts was analyzed using a wide-angle X-ray diffractometer (Rigaku SmartLab) employing Cu K_α radiation (λ = 0.15418 nm). Scanning electron microscope (SEM) imaging of samples was performed using a FEI F50 SEM. Diffuse reflectance of samples was measured with a JASCO V-670 UV-Vis-NIR spectrophotometer. The photoluminescence (PL) spectra were recorded on a PL spectrofluorometer (Horiba Jobin) at an excitation wavelength of 365 nm.

2.4. Photocatalytic evaluation

The degradation of RhB was used as a model reaction to evaluate photodegradation behavior of the ternary Ag/Ag_3PO_4/g-C_3N_4 hybrid photocatalyst. For the photodegradation experiments, a 150 mL solution of RhB (7 mg/L) was prepared, into which 150 mg of photocatalyst was added. The suspension of the RhB solution and photocatalyst was magnetically stirred in the dark for 60 min to ensure adsorption-desorption equilibrium before the irradiation. The suspension was then irradiated with a 300 W Xenon lamp equipped with visible light band pass filter (400–800 nm). Portions of the reaction mixture slurry were taken from the mixture and filtered to remove Ag/Ag_3PO_4/g-C_3N_4 hybrid photocatalyst at regular intervals. The concentration of RhB in the aqueous solution was determined using a UV-VIS spectrophotometer (Hitachi U-3900).

3. Results and discussion

3.1. Structure and composition of synthesized catalysts

Figure 1 depicts XRD patterns of the ternary Ag/Ag_3PO_4/g-C_3N_4 hybrid photocatalyst prepared at different exposure time. The diffraction peaks of both g-C_3N_4 and silver nanoparticles cannot be observed clearly in XRD patterns because of strong interference with the Ag_3PO_4 signals. However, a new peak appeared at 38.1° in the Ag_3PO_4/g-C_3N_4 sample irradiated for 3 h that could be indexed as the silver (111).

The enlarged XRD patterns (Fig. 2) from 37° to 40° and 26.5° to 29° show the Ag(111) and g-C_3N_4 (002) peaks, respectively. These results confirmed the formation of silver particles on the surface of the Ag_3PO_4 particles and the existence of a g-C_3N_4 phase. The diffraction intensity of the Ag(111) peak

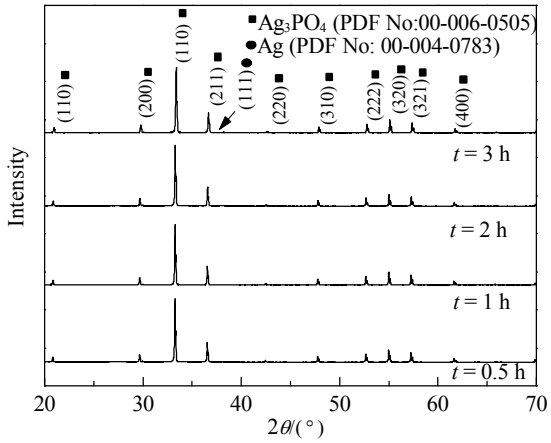

Fig. 1. XRD patterns of series ternary Ag/Ag_3PO_4/g-C_3N_4 hybrid photocatalysts prepared under visible light exposure for 0.5, 1, 2, and 3 h.

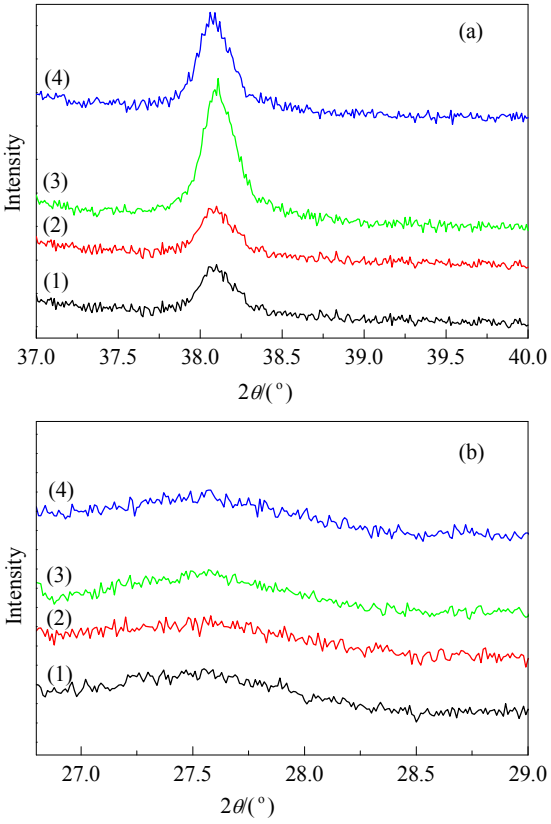

Fig. 2. Enlarged XRD patterns of Ag(111) (a) and g-C_3N_4(002) (b) diffraction peaks from series ternary Ag/Ag_3PO_4/g-C_3N_4 photocatalysts prepared under visible light exposure for 0.5 (1), 1 (2), 2 (3), and 3 h (4).

increased and saturated with prolonged irradiation time, which may suggest that the silver nanoparticles formed in situ on surface of Ag_3PO_4 and inhibited further photochemical reduction of the Ag_3PO_4 to Ag^0. The size of the silver nanoparticles from different light exposed samples was calculated and summarized in Table 1 using the Scherrer equation based on full width at half maximum (FWHM) value for Ag(111) peak at 38.1°. By a semi quantitative analysis, 0.6%, 1.0%, 2.1%, and 2.8% metallic silver was estimated in samples irradiated for

Table 1
Calculated particle sizes and composition ratios of silver nanoparticles.

t/h	FWHM (Ag(111))/(°)	Particle size (nm)	*w*(Ag)/%
0.5	0.220	39.7	0.6
1	0.241	36.0	1.0
2	0.245	35.5	2.1
3	0.232	37.6	2.8

0.5, 1, 2, and 3 h, respectively. Figure 3 shows a typical SEM image of Ag/Ag_3PO_4/g-C_3N_4 (0.8; 1 h) photocatalyst. The silver nanoparticles can be clearly seen in the SEM images, and the particle size is estimated at around 40–50 nm, which is in agreement with the XRD analysis.

3.2. *Optical properties of synthesized photocatalysts*

Figure 4 illustrates the optical absorption spectra of g-C_3N_4, Ag_3PO_4, Ag_3PO_4/g-C_3N_4 (0.8), and Ag/Ag_3PO_4/g-C_3N_4 (0.8; 1 h). The peaks at around 393 and 454 nm in the ternary Ag/Ag_3PO_4/g-C_3N_4 hybrid photocatalyst can be attributed to the absorptions of g-C_3N_4 and Ag_3PO_4, respectively. Ag/Ag_3PO_4/g-C_3N_4 exhibits much higher absorption, which may be attributed to the surface plasmon resonance (SPR) of the silver nanoparticles [23].

PL spectra of g-C_3N_4 and Ag/Ag_3PO_4/g-C_3N_4 (0.8; *t*) samples

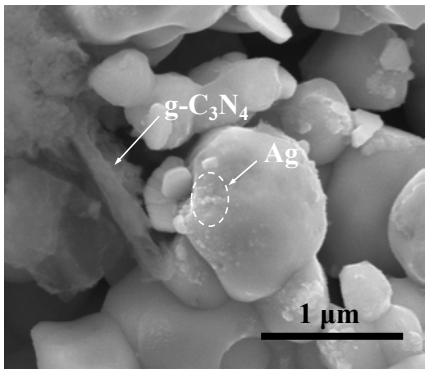

Fig. 3. SEM image of as-prepared ternary Ag/Ag_3PO_4/g-C_3N_4 (0.8; 1 h) hybrid photocatalyst.

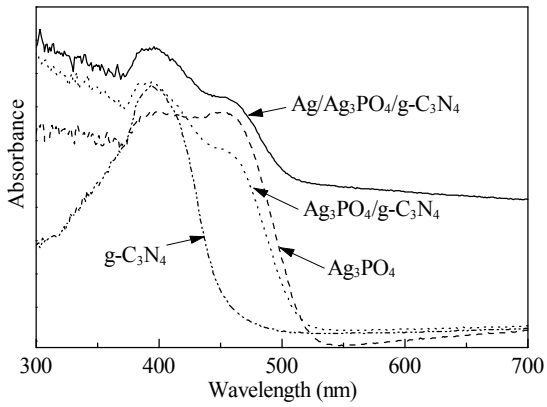

Fig. 4. UV-Vis absorption spectra of ternary Ag/Ag_3PO_4/g-C_3N_4 (0.8; 1 h) hybrid photocatalyst, binary Ag_3PO_4/g-C_3N_4 (0.8) photocatalyst, Ag_3PO_4, and g-C_3N_4.

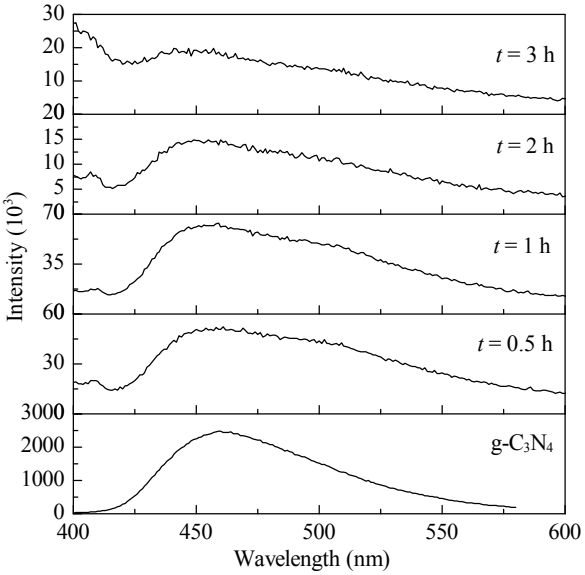

Fig. 5. PL spectra of series ternary $Ag/Ag_3PO_4/g\text{-}C_3N_4$ (0.8; *t*) hybrid photocatalysts and $g\text{-}C_3N_4$ semiconductor.

are shown in Fig. 5. A strong emission band centered at 459 nm in $g\text{-}C_3N_4$ can be assigned to the emission of $g\text{-}C_3N_4$ with an energy corresponding to its band gap. This indicates more efficient radiative recombination of the photogenerated carriers inside the $g\text{-}C_3N_4$ semiconductor in samples prepared with longer irradiation time. The overall PL emission intensity of the $Ag/Ag_3PO_4/g\text{-}C_3N_4$ (0.8; *t*) hybrid photocatalysts decreased with respect to the overall PL intensity of $g\text{-}C_3N_4$ with increasing irradiation time. This may be attributed to charge transfer between Ag_3PO_4 and $g\text{-}C_3N_4$ or trapping of photoexcited electrons by the silver nanoparticles.

3.3. Photocatalytic activity

The effect of the Ag_3PO_4/C_3N_4 mass ratio from Ag_3PO_4 to $g\text{-}C_3N_4$ on the photodegradation performance was investigated before studying the enhancement of photodegradation by the silver nanoparticles in the ternary systems. Figure 6 illustrates the photocatalytic activity of a series of Ag_3PO_4/C_3N_4 hybrid photocatalysts investigated. The $Ag_3PO_4/g\text{-}C_3N_4$ hybrid photocatalysts showed considerably enhanced photocatalytic performance compared with either Ag_3PO_4 or $g\text{-}C_3N_4$ alone, suggesting a synergic effect as reported by Zhang et al. [24] and Kumar et al. [25]. The optimum composition ratio was found to be 4:1 for the $Ag_3PO_4/g\text{-}C_3N_4$ hybrid, and this photocatalyst completely decomposed the model contaminant over the course of the experiment. Only 63% and 12% degradation of RhB were observed within 30 min using pure Ag_3PO_4 and $g\text{-}C_3N_4$, respectively.

The curves in Fig. 7 depict the removal of RhB as a function of irradiation time using the ternary $Ag/Ag_3PO_4/g\text{-}C_3N_4$ hybrid photocatalysts. Further enhancement in photodegradation performance was observed from the as-prepared $Ag/Ag_3PO_4/g\text{-}C_3N_4$ samples. Almost 50% of the RhB in the aqueous suspension was decomposed using $Ag/Ag_3PO_4/g\text{-}C_3N_4$ (0.8; 1 h) under

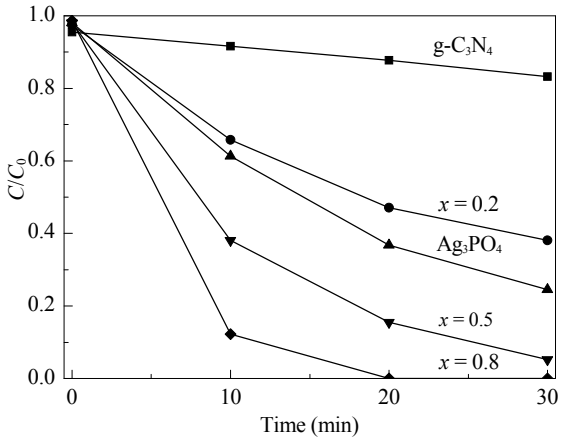

Fig. 6. Changes of RhB concentration over a series of binary $Ag_3PO_4/g\text{-}C_3N_4$ (x = 0, 0.2, 0.5, 0.8, 1) photocatalysts.

broadband visible light irradiation for 5 min. This ratio may be considered as the optimal compositional ratio of the ternary photocatalyst. Around 40% degradation was obtained from $Ag_3PO_4/g\text{-}C_3N_4$ (0.8) under identical experimental conditions.

The corresponding UV-Vis spectral changes (inset in Fig. 7) show the intensity of the absorption peak at 554 nm decreasing dramatically as the photodegradation reaction progresses. It is notable that no blue-shift of the RhB absorption peak centered at 554 nm was observed, suggesting a decomposition mecha-

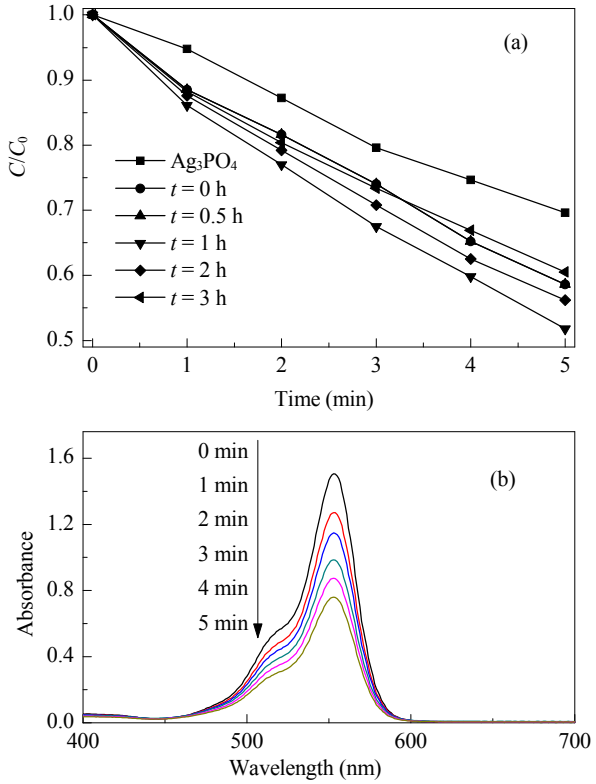

Fig. 7. (a) Changes of the RhB concentration over series ternary $Ag/Ag_3PO_4/g\text{-}C_3N_4$ (0.8; *t*) hybrid photocatalysts; (b) Changes to the UV-Vis spectra of the RhB with $Ag/Ag_3PO_4/g\text{-}C_3N_4$ (0.8; 1 h) as a function of irradiation time.

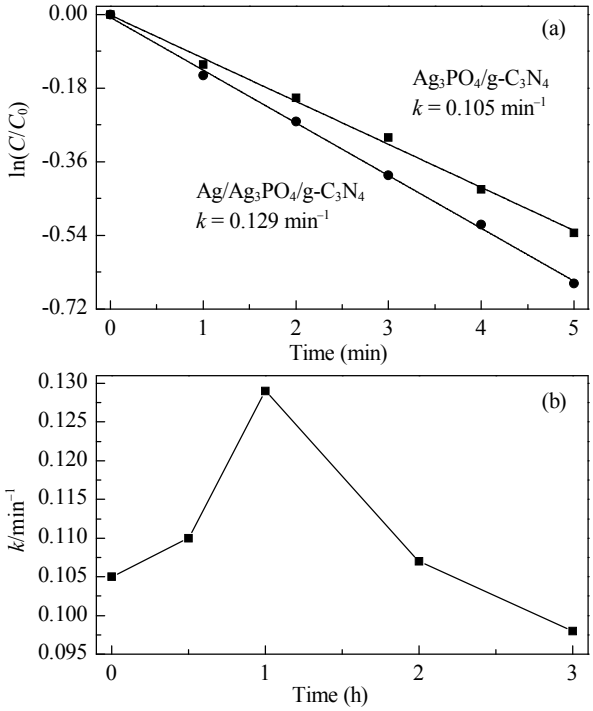

Fig. 8. (a) Comparison of rate constants (fitted by pseudo-1st-order kinetic model) of $Ag_3PO_4/g\text{-}C_3N_4$ (0.8) and as-prepared $Ag/Ag_3PO_4/g\text{-}C_3N_4$ (0.8; 1 h) hybrid photocatalyst. (b) Changes of rate constants on the irradiation time in the preparation of $Ag/Ag_3PO_4/g\text{-}C_3N_4$ (0.8; 0–3 h).

nism involving cleavage of the whole conjugated chromophore structure in RhB during the photochemical reaction, rather than an N-deethylation process [26].

Figure 8 shows a comparison of the apparent rate constants (k) of the $Ag/Ag_3PO_4/g\text{-}C_3N_4$ (0.8; 1 h) hybrid photocatalysts and $Ag_3PO_4/g\text{-}C_3N_4$ calculated by the Langmuir-Hinshelwood model [27]. Using the binary $Ag_3PO_4/g\text{-}C_3N_4$ photocatalyst as a baseline, an apparent rate of 0.105 min^{-1} was obtained for the reaction in the first 5 min. The $Ag/Ag_3PO_4/g\text{-}C_3N_4$ hybrid photocatalyst prepared by light irradiation for 1 h showed a 25% enhancement (0.129 min^{-1}). Figure 8 (b) shows the effect of irradiation time during the preparation of $Ag/Ag_3PO_4/g\text{-}C_3N_4$ (i.e. which correlates with the loading of silver nanoparticles) on the kinetic rate constant. It is clear that the kinetic rate constant increases initially with the silver nanoparticle loading and subsequently decreases. The highest performance was obtained from $Ag/Ag_3PO_4/g\text{-}C_3N_4$ (0.8; 1 h).

Compared with other popular photocatalytic systems, the as-prepared ternary $Ag/Ag_3PO_4/g\text{-}C_3N_4$ (0.8; 1 h) hybrid photocatalyst exhibits superior performance. A comparison shown in Fig. 9 suggests that the kinetic rate constant of $Ag/Ag_3PO_4/g\text{-}C_3N_4$ (0.8; 1 h) at 0.129 min^{-1} within 6 min is higher than the kinetic rate constants observed on anatase TiO_2 (0.009 min^{-1}), P25 (0.016 min^{-1}), $NaBiO_3$ (0.054 min^{-1}), Ag_3PO_4 (0.073 min^{-1}), and $Ag_3PO_4/g\text{-}C_3N_4$ (0.8) (0.105 min^{-1}). The low photodegradation rate of RhB on TiO_2 (or P25) may be attributed to the wide band gap of the materials, which restricts photosensitization by visible light [28]. Compared with the commercial photocatalyst

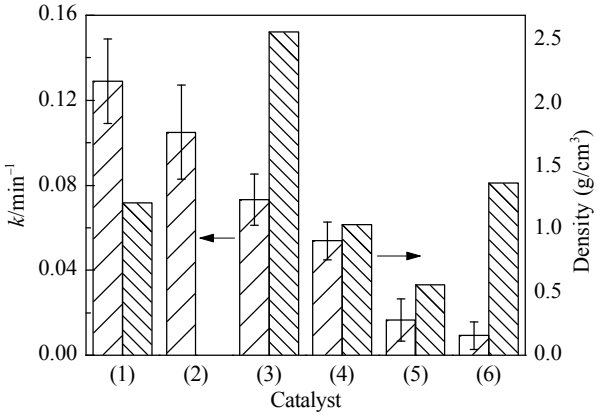

Fig. 9. Comparison of photocatalytic performance and solid density of various photocatalysts. (1) $Ag/Ag_3PO_4/g\text{-}C_3N_4$; (2) $Ag_3PO_4/g\text{-}C_3N_4$; (3) Ag_3PO_4; (4) $NaBiO_3$; (5) P25; (6) Anatase TiO_2.

P25, a 6-fold improvement of photodegradation activity was achieved for the $Ag/Ag_3PO_4/g\text{-}C_3N_4$ (0.8; 1 h) hybrid photocatalyst. In addition, as shown in Fig. 9, the high density of the hybrid photocatalyst (ρ = 1.2 g/cm^3) indicates that it would be more convenient to separate it from the aqueous phase for regeneration and reuse, compared with P25 (ρ = 0.56 g/cm^3).

The proposed ternary $Ag/Ag_3PO_4/g\text{-}C_3N_4$ hybrid photocatalyst can be easily recycled using a simple filtration technique and then washed with water to remove adsorbed RhB. As depicted in Fig. 10, after the first three cycles, the kinetic rate constants remained above 0.12 min^{-1}. The kinetic constant rate decreased to 0.04 min^{-1} after the 6th cycle, likely because of catalyst fouling [29].

3.4. Possible mechanisms of decomposition

The adsorption of RhB molecules to the Ag_3PO_4 or $g\text{-}C_3N_4$ photocatalyst surfaces was investigated, revealing that less than 4% of the RhB adsorbed to Ag_3PO_4 or $g\text{-}C_3N_4$. The weak interaction of the RhB with this material may be considered one of the reasons for the enhanced photoactivity following introduction of silver nanoparticles. It is also notable that the enhancement in activity arises from the bifunctional heterojunction structure at the interface of $Ag_3PO_4/g\text{-}C_3N_4$, as indi-

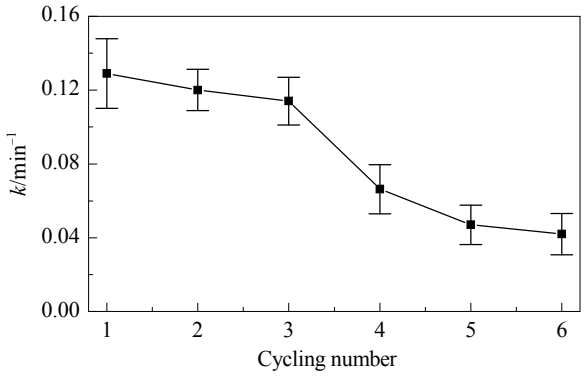

Fig. 10. Changes of the rate constant (fitted by pseudo-1st-order kinetic model) of RhB decomposition on ternary $Ag/Ag_3PO_4/g\text{-}C_3N_4$ (0.8; 1 h) over six successive photodegradation cycles.

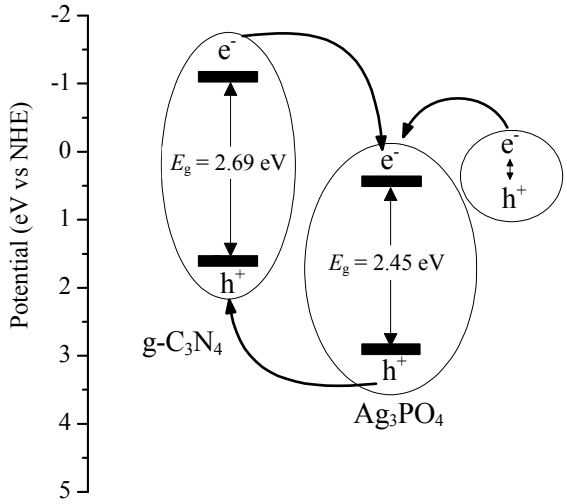

Fig. 11. Possible mechanism of photoactivity enhancement onto ternary Ag/Ag_3PO_4/g-C_3N_4 hybrid photocatalyst by fast separation of carriers.

cated by PL data and the SPR from the silver nanoparticles of the ternary Ag/Ag_3PO_4/g-C_3N_4 hybrid photocatalyst. The proposed mechanism of charge carrier separation in system is illustrated in Fig. 11.

It is reported [24,25] that the conduction band edges of g-C_3N_4 and Ag_3PO_4 are at −1.12 eV and 0.45 eV (vs NHE), respectively. Thus photoexcited electrons from the conduction band (CB) of g-C_3N_4 are injected into the CB of Ag_3PO_4 because of favorable offset between the CB edges of g-C_3N_4 and Ag_3PO_4 as illustrated in Fig. 11. The photogenerated holes move from the valance band (VB) of the Ag_3PO_4 towards the VB of g-C_3N_4 because of the more positive VB edge of Ag_3PO_4 (2.9 eV, vs NHE) than that of g-C_3N_4 (1.57 eV, vs NHE).

Harnessing the plasmonic effects of silver nanoparticles, to generate highly-active composite photocatalysts through combining the nanoparticles with semiconducting materials has been reported including Ag-TiO_2 nanocomposite hollow spheres [30] and Ag/AgCl/TiO_2 nanotube arrays [31], etc. Our previous simulation results [32] have clearly shown that the highest surface plasmon polariton momentum of silver nanoparticles is achieved by irradiation of photons with a wavelength of 359 nm in RhB aqueous solution, by considering the Brendel-Bormann model. The surface plasmon polariton momentum is decreased by 25% when changing the wavelength of the excitation source from 359 to 400 nm. This may also explain why the apparent photocatalytic enhancement of the Ag/Ag_3PO_4/g-C_3N_4 hybrid photocatalyst can be observed under visible light irradiation between 400 and 800 nm, even though the most efficient excitation wavelength for the SPR effect is λ = 359 nm, which has a naturally low intensity in the solar spectrum. Decreased catalytic activity was observed for samples that were highly decorated with silver nanoparticles. Further reduction of silver on the surface of Ag_3PO_4 not only destroyed the SPR because of agglomeration of silver nanoparticles but also reduced the surface area available for the reaction on Ag_3PO_4.

4. Conclusions

The preparation of a ternary Ag/Ag_3PO_4/g-C_3N_4 hybrid photocatalyst and its improved photodegradation performance are reported. The highest photoactivity was achieved by optimization of the silver nanoparticle (w = 1.0%) surface coverage on the Ag_3PO_4 and the composition fraction (x = 0.8) of Ag_3PO_4 and g-C_3N_4. The as prepared hybrid photocatalyst can be regenerated and separated from the aqueous phase easily. In addition, the catalyst also exhibits high photostability under visible light exposure and shows enhanced photodegradation of RhB dye in solution compared with other typical photocatalysts.

References

[1] Fujishima A, Honda K. *Nature*, 1972, 238: 37
[2] Asahi R, Morikawa T, Ohwaki T, Aoki K, Taga Y. *Science*, 2001, 293: 269
[3] Zou Z G, Ye J H, Sayama K, Arakawa H. *Nature*, 2001, 414: 625
[4] Kudo A, Miseki Y. *Chem Soc Rev*, 2009, 38: 253
[5] Zhang Y, Pan Z M, Wang X C. *Chin J Catal* (郑云, 潘志明, 王心晨. 催化学报), 2013, 34: 524
[6] Wang W, Lu C H, Su M X, Ni Y R, Xu Z Z. *Chin J Catal* (王卫, 陆春华, 苏明星, 倪亚茹, 许仲梓. 催化学报), 2012, 33: 629
[7] Yi Z G, Ye J H, Kikugawa N, Kako T, Ouyang S X, Stuart-Williams H, Yang H, Cao J Y, Luo W J, Li Z S, Liu Y, Withers R. *Nat Mater*, 2010, 9: 559
[8] Umezawa N, Ouyang S X, Ye J H. *Phys Rev B*, 2011, 83: 035202
[9] Wang X C, Maeda K, Thomas A, Takanabe K, Xin G, Carlsson J M, Domen K, Antonietti M. *Nat Mater*, 2009, 8: 76
[10] Pan C S, Xu J, Wang Y J, Li D, Zhu Y F. *Adv Funct Mater*, 2012, 22: 1518
[11] Xiang Q J, Yu J G, Jaroniec M. *J Phys Chem C*, 2011, 115: 7355
[12] Ge L, Han C C, Liu J. *Appl Catal B*, 2011, 108-109: 100
[13] Shiravand G, Badiei A, Ziarani G M, Jafarabadi M, Hamzehloo M. *Chinese J Catal* (催化学报), 2012, 33: 1347
[14] Pan H Q, Li X K, Zhuang Z J, Zhang C. *J Mol Catal A*, 2011, 345: 90
[15] Yan S C, Lü S B, Li Z S, Zou Z G. *Dalton Trans*, 2010, 39: 1488
[16] Gondal M A, Rashid S G, Dastageer M A, Zubair S M, Ali M A, Lienhard J H, McKinley G, Varanasi K K. *IEEE Photonics J*, 2013, 5: 2201908
[17] Gondal M A, Ali M A, Dastageer M A, Chang X F. *Catal Lett*, 2013, 143: 108
[18] Shen K., Gondal M A, Li Z J, Li L Y, Xu Q Y, Yamani Z H. *React Kinet Mechan Catal*, 2013, 109: 247
[19] Zhang J, Gondal M A, Wei W, Zhang T N, Xu Q Y, Shen K. *J Alloys Compd*, 2012, 530: 107
[20] Luo L R, Shen K, Xu Q Y, Zhou Q, Wei W, Gondal M A. *J Alloys Compd*, 2013, 558: 73
[21] Zhang B, Ji G B, Gondal M A, Liu Y S, Zhang X M, Chang X F, Li N W. *J Nanopart Res,* 2013, 15: 1773
[22] Yan S C, Li Z S, Zou Z G. *Langmuir*, 2009, 25: 10397
[23] Bhui D K, Bar H, Sarkar P, Sahoo G P, De S P, Misra A. *J Mol Liq*, 2009, 145: 33
[24] Zhang F J, Xie F Z, Zhu S F, Liu J, Zhang J, Mei S F, Zhao W. *Chem Eng J*, 2013, 228: 435
[25] Kumar S, Surendar T, Baruah A, Shanker V. *J Mater Chem A*, 2013, 1: 5333
[26] Wang Q, Chen C C, Zhao D, Ma W H, Zhao J C. *Langmuir*, 2008, 24:

Graphical Abstract

Chin. J. Catal., 2014, 35: 78–84 doi: 10.1016/S1872-2067(12)60712-8

Preparation of ternary Ag/Ag_3PO_4/g-C_3N_4 hybrid photocatalysts and their enhanced photocatalytic activity driven by visible light

Kai Shen*, Mohammed Ashraf Gondal*, Rashid Ghulam Siddique, Shan Shi, Siqi Wang, Jiangbo Sun, Qingyu Xu
Nanjing University of Aeronautics and Astronautics, China;
King Fahd University of Petroleum and Minerals, Saudi Arabia;
Southeast University, China

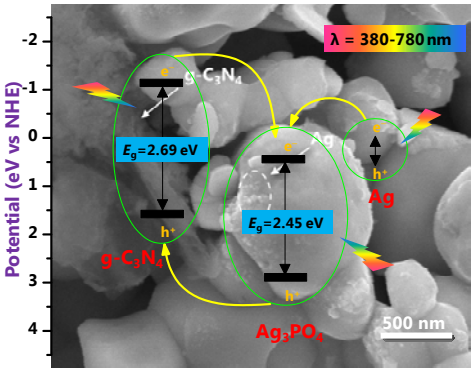

Ternary Ag/Ag_3PO_4/g-C_3N_4 photocatalyst exhibits excellent photocatalytic activity driven by visible light, attributed to surface plasmon resonance of 40 nm-silver nanoparticles formed on the surface of Ag_3PO_4, and the heterojunction at the interface between Ag_3PO_4 and g-C_3N_4.

7338
[27] Park C Y, Ghosh T, Meng Z D, Kefayat U, Vikram N, Oh W C. *Chin J Catal* (催化学报), 2013, 34: 711
[28] Chen C C, Ma W H, Zhao J C. *Chem Soc Rev*, 2010, 39: 4206
[29] Wang W G, Cheng B, Yu J G, Liu G, Fan W H. *Chem Asian J*, 2012, 7: 1902
[30] Xiang Q J, Yu J G, Cheng B, Ong H C. *Chem Asian J*, 2010, 5: 1466
[31] Yu J G, Dai G P, Huang B B. *J Phys Chem C*, 2009, 113: 16394
[32] Gondal M A, Chang X F, Sha W E I, Yamani Z H, Zhou Q. *J Colloid Interf Sci*, 2013, 392: 325

Ag/Ag_3PO_4/g-C_3N_4三元复合光催化剂的制备及其可见光驱动下的光催化活性增强

沈　凯[a,*], Mohammed Ashraf Gondal[b,#], Rashid Ghulam Siddique[b],
施　珊[a], 王斯琦[a], 孙江波[a], 徐庆宇[c]
[a]南京航空航天大学材料科学与技术学院, 江苏南京211100
[b]法赫德国王石油与矿业大学物理系, 达兰31261, 沙特阿拉伯
[c]东南大学物理系, 江苏南京211189

摘要: 报道了一种新型Ag/Ag_3PO_4/g-C_3N_4三元复合光催化剂的制备及其半导体界面处的快速载流子分离所引起的光催化活性的显著增强效应. 通过X射线衍射, 扫描电子显微镜, 紫外-可见吸收光谱以及光致发光光谱等就其晶体结构、形貌、组分、光学吸收以及载流子的快速分离行为进行了表征与分析. 以罗丹明B作为模型化合物分子, 研究发现, 所制备的Ag/Ag_3PO_4/g-C_3N_4三元复合光催化剂在可见光照射下表现出比Ag_3PO_4以及Ag_3PO_4/g-C_3N_4二元催化剂更为优异的光催化活性. 研究认为, Ag_3PO_4表面尺寸约为40 nm的Ag纳米粒子在可见光下受激所产生的等离子表面共振效应以及Ag_3PO_4与g-C_3N_4界面处所形成的类似异质结结构对所制备的Ag/Ag_3PO_4/g-C_3N_4三元复合光催化剂光催化活性的显著增强起到重要作用.

关键词: 银纳米粒子; 磷酸银; 石墨型氮化碳; 表面等离子共振; 异质结

收稿日期: 2013-07-26. 接受日期: 2013-09-10. 出版日期: 2014-01-20.
*通讯联系人. 电话: (025)84895871; 传真: (025)84895871; 电子信箱: shenkai84@nuaa.edu.cn
#通讯联系人. 电话: +966-3-8602351; 传真: +966-3-8604281; 电子信箱: magondal@kfupm.edu.sa
基金来源: 国家自然科学基金(51172044); 阿拉伯法赫德国王石油矿产大学-美国麻省理工学院国际合作基金(R15-CW-11, MIT11109, MIT11110).
本文的英文电子版由Elsevier出版社在ScienceDirect上出版(http://www.sciencedirect.com/science/journal/18722067).